

Spontaneous Growth of Au Nanoparticles onto CdS, ZnS or PbS Thin Films for Electrochemical Immunosensors

Hongcheng Pan^{1,2,3,*}, Shan Huang¹, Xuepeng Li¹, Ping Li¹ and Wenyuan Zhu⁴

¹ College of Chemistry and Bioengineering, Guilin University of Technology, 12 Jiangan Road, Guilin 541004, P. R. China.

² Guangxi Colleges and Universities Key Laboratory of Food Safety and Detection, Guilin University of Technology, 12 Jiangan Road, Guilin 541004, P. R. China.

³ Guangxi Key Laboratory of Electrochemistry and Magnetochemistry Functional Materials, Guilin University of Technology, 12 Jiangan Road, Guilin 541004, P. R. China.

⁴ Collaborative Innovation Center for Water Pollution Control and Water Safety in Karst Area, Guilin University of Technology, Guilin 541004, P. R. China

*E-mail: hcp@163.com

Received: 15 February 2016 / Accepted: 29 March 2016 / Published: 1 April 2016

A facile method to fabricate Au-CdS (or ZnS, PbS) nanocomposites is reported. The method is based on spontaneous growth of Au onto the metal sulfide nanoparticles. Unlike typical synthesis of Au-semiconductor nanocomposites, this method does not require additional steps of introducing other reducing agents. Direct redox reactions occurs between Au(III) ions and metal sulfide nanoparticles. We have probed the Au-semiconductor nanocomposites by scanning electron microscopy (SEM), transmission electron microscopy (TEM), and X-ray diffraction (XRD). A possible mechanism was proposed for spontaneous growth of Au nanoparticles. It was found that H₂O₂ appeared to inhibit the Au growth onto the metal sulfide surface. We accordingly developed an enzyme-linked sandwich electrochemical immunosensor for the detection of human immunoglobulin G (IgG). In the electrochemical immunosensor, we use the glucose oxidase labeled antibody to generate H₂O₂ that inhibits the Au growth on CdS films, thereby decreasing the cathodic current at 0.9 V. This immunosensor can detect IgG as low as 1.5 ng/mL.

Keywords: Spontaneous growth; Au-CdS nanocomposites; metal sulfide

1. INTRODUCTION

Growing Au nanoparticles onto semiconductor substrates has attracted considerable interest in recent years[1-9]. The interactions between the plasmonic gold and semiconductor substrates can

significantly improve the performance of the Au-semiconductor nanosystems and can even generate new properties[10]. For instance, gold and semiconductor would form Schottky barriers at their interfaces, leading to separation and transfer of photoinduced charges. Such an effect would be especially important for photocatalysis and luminescence[5]. Furthermore, the growth of Au nanoparticles was used as a method for signal amplification of biosensors[11, 12].

In the past two decades, considerable efforts have been devoted to developing strategies for construction of Au nanoparticles-semiconductor nanocomposites. Among these successful synthesis routes, the site-selective gold deposition onto the semiconductor component is widely used. This method is well exemplified by the growth of Au nanoparticles on the apex of cadmium chalcogenide nanorods. In this method, Au ions in solution were reduced, followed by their accumulation at lattice defects resulted in the formation of small gold islands along lateral surfaces, as well as larger gold domains at both Se (S) and Cd-rich facets of CdSe (S) nanorods. By improving the charge separation and enhancing the light absorption, gold ingredients in gold-semiconductor nanostructures can improve the photocatalytic and light-harvesting efficiencies of semiconductors[4, 7-9].

Recently, the growth of gold have been used to amplify the biosensing signals. The catalytic enlargement of Au nanoparticles, acting as labels for DNA hybridization, was used for the amplified microgravimetric quartz-crystal-microbalance detection of nucleic acids[13, 14]. Willner and coworkers[15-17] reported that the coupling of enzymes to the biocatalytic growth of Au nanoparticles was employed for the signal amplification of biosensors. Rica and Stevens have developed a signal generation approach for the enzyme-linked immunosorbent assay (ELISA) [18]. This method is based on the enzyme-controlled growth of Au nanoparticles and enables the detection of a few molecules of analyte with the naked eye. Our group recently developed a versatile strategy for electrochemical and optical signal-on/off immunosensing, on the basis of enzyme-mediated growing Au nanoparticles[12]. By applying antibody and enzyme (glucose oxidase or catalase) conjugated Au nanoparticles as secondary antibodies, the sandwich-type immunosensor can achieve either a "signal-on" or a "signal-off" detection. The Au nanoparticles growth is dependent on H_2O_2 concentration, which is mediated by glucose oxidase or catalase. More Au nanoparticles lead to larger electrochemical and optical signals, and vice versa.

The growth of Au nanoparticles typically involves adding reducing agents to reduce Au(III) to Au(0). However, it may yield high background signals and false positive results. Here we report a spontaneous growth of Au nanoparticles onto CdS, ZnS or PbS thin films for electrochemical immunosensors.

2. EXPERIMENTAL

2.1. Chemicals and materials

$CdCl_2$, $ZnSO_4$, $PbAC_2$ and $HAuCl_4 \cdot 4H_2O$ was purchased from Sinopharm (Shanghai, China). Cetyltrimethylammonium chloride (CTAC), thiourea, and ammonia were obtained from Beijing Chemical Reagent (Beijing, China). Human immunoglobulin G (IgG), goat-anti-human IgG antibody (Ab1), and monoclonal mouse-anti-human IgG antibody (Ab2) were supplied by Baoman biotechnology (Shanghai, China). Glucose oxidase (GOx) was obtained from Hualan Chemical

(Shanghai, China). Indium-tin-oxide-coated (ITO) glass electrodes ($7 \Omega/\square$, $13 \times 30 \times 1.1$ mm) were from Kaivo Optoelectronic (Zhuhai, China). Other reagents were of analytical grade. Ultrapure water (resistivity $>18 \text{ M}\Omega \text{ cm}$) was obtained from a WP-UP-IV-30 purification system (Woter, China) and used in the all experiments.

2.2. Deposition of CdS, ZnS, and PbS thin films on ITO-coated glass substrates

CdS, ZnS, and PbS nanoparticles were deposited by a chemical bath deposition (CBD) method onto ITO-coated glass substrates[19-21]. The CBD process is based on the reaction of metal salts (CdCl_2 , ZnSO_4 , and PbAC_2) with thiourea and ammonia in an aqueous solution. For the deposition of CdS nanoparticles, the solution contains: 18 mL of ultrapure water, 15 mL of 5 mM CdCl_2 , 5 mL of 0.05 M tri-sodium citrate, 8 mL of 2.6% (w/w) ammonia, and 4 mL of 0.05 M thiourea. For the deposition of ZnS nanoparticles, the solution contains: 39.25 mL of ultrapure water, 2.5 mL of 0.5 M PbAC_2 , 1 mL of 1 M triethanolamine, 1.25 mL of 1 M NaOH, and 6 mL of 0.5 M thiourea. The nanoparticles were deposited onto ITO slides, which were cleaned by sequential ultrasonic cleaning in acetone, ethanol, and ultrapure water for 5 min each, and drying in air. The ITO slides were immersed in the solution and then were heated to the required temperature ($83 \text{ }^\circ\text{C}$ for CdS, $90 \text{ }^\circ\text{C}$ for ZnS, and $50 \text{ }^\circ\text{C}$ for PbS, respectively) and maintained here for 3 h. After the ITO substrates were removed, they were rinsed and ultrasonically cleaned in ultrapure water to remove loose particles from the surface and then dried in air. These CdS-, ZnS-, and PbS-deposited ITO slides are hereinafter referred to as CdS/ITO, ZnS/ITO, and PbS /ITO, respectively..

2.3. Spontaneous growth of Au nanoparticles onto MS/ITO ($M = \text{Cd, Zn, and Pb}$)

The MS/ITO slides was immersed in a solution (diluted to a total volume of 10 mL with ultrapure water) containing 0.3 mL of 0.2 M phosphate buffer solution (PBS, pH 6.0), 100 μL of 1% (w/w) HAuCl_4 , and 80 μL of 0.2 M CTAC for 3 h at $37 \text{ }^\circ\text{C}$ and subsequently rinsed with ultrapure water. The Au nanoparticles spontaneous deposited CdS/ITO, ZnS/ITO, and PbS /ITO are hereinafter referred to as Au-CdS/ITO, Au-ZnS/ITO, and Au-PbS /ITO, respectively.

2.4. Synthesis of citric-coated Au nanoparticles (AuNPs) and preparation of GOx-Ab2-AuNP bioconjugates

GOx-Ab2-AuNP bioconjugates were prepared according to our previous report[12]. Briefly, 10 μL of 1.0 mg/mL Ab2 was added to 3 mL of citric-coated AuNPs (~ 25 nm in diameter) solution in a 5-mL centrifuge tube, followed by vortex-mixing for 120 min. The solution was centrifuged at 15000 revolutions per minute (rpm) for 20 min. To the precipitates was added 1.5 mL of a solution containing 0.5 mg/mL GOx and 5 mM phosphate-buffered saline (PBS, pH 6.8). The solution was incubated overnight at $4 \text{ }^\circ\text{C}$, followed by addition 50 μL of BSA solution (2%, w/w). After vortex-mixing for 30 min, the solution was centrifuged at 15000 rpm for 20 min. Precipitates were washed twice with 1.0

mL of BSA solution (1%, w/w), centrifuging 20 min at 15000 rpm with each wash. The precipitates were resuspended in 0.5 mL of BSA solution (1%, w/w).

2.5. Fabrication of immunosensor

A 10- μ L of 400 μ g/mL Ab1 solution (containing 0.05 M PBS, pH 6.0) was dropped and spread on the conductive surface of the CdS/ITO electrode. The Ab1-coated electrode was incubated at 4 °C for 8 h in air at saturation humidity, followed by rinsing with a mixture of 0.05 M PBS (pH 7.4) and 0.05% Tween-20 (v/v). The air-dried electrode was blocked with 2% BSA solution (w/w) to avoid non-specific adsorption.

2.6. Immunoassay procedures and growth of AuNPs

The immunosensor was immersed in a solution containing 0.05 M pH 7.4 PBS, 0.1% BSA, 0.05% Tween-20, and desired amount of IgG and incubated at 37 °C for 50 min. After rinsing with 0.05 M PBS (pH 7.4, containing 0.05% Tween-20), the immunosensor was immersed in a solution containing 20 μ L of GOx-Ab2-AuNPs. Finally, the immunosensor was washed thoroughly with 0.05 M PBS (pH 7.4, containing 0.05% Tween-20) and ultrapure water to remove non-specifically bound bioconjugates.

2.7. Characterization and electrochemical measurements

The surface morphology and microstructure of the immunosensors were observed with a Hitachi S-4800 scanning electron microscope (SEM). X-ray Power diffraction (XRD) measurements were carried out on an X-ray diffractometer (X'pert PRO, Philips, Eindhoven, Netherlands). High-resolution transmission electron microscopy (HRTEM) was carried out using a FEI Tecnai G2 F20 S-Twin microscope. UV-vis absorption spectra were recorded on a Cary 50 spectrophotometer (Varian, USA). Differential pulse voltammetry (DPV) measurements were carried out on a CHI 660B electrochemical workstation (Ch Instruments, China) with a conventional three-electrode system consisting of a modified ITO electrode as the working electrode, an Ag/AgCl (saturated KCl) electrode as the reference electrode, and a Pt wire electrode as the counter electrode. DPV experiments were performed with a 0.5 M H₂SO₄ solution. All potentials are reported versus the Ag/AgCl (saturated KCl) reference at room temperature.

3. RESULTS AND DISCUSSION

3.1. Deposition of CdS, ZnS, and PbS nanoparticles onto ITO substrates

CdS, ZnS, and PbS nanoparticles were deposited onto ITO-coated glass substrates by a chemical bath deposition (CBD) method [19-21]. The CBD process is based on the reaction of metal salts (CdCl₂, ZnSO₄, and PbAc₂) with thiourea and ammonia in an aqueous solution. The compact and

uniform thin films were grown onto the substrates after the deposition. The deposited ITO slides are hereinafter referred to as CdS/ITO, ZnS/ITO, and PbS /ITO.

The surface morphology of chemical-bath-deposited CdS, ZnS, and PbS thin films were characterized by SEM (Figure 1). The CdS film consists of densely packed spherical grains with diameters of 60-100 nm (Figure 1(a)). The ZnS film is composed of larger crystalline particles (typically 150-300 nm in size) than the CdS film. Most of crystalline particles have coalesced to form a continuous film. The PbS thin film is composed of cubic-shaped PbS nanocrystals (about 70 nm in size) as shown in Figure 1(c).

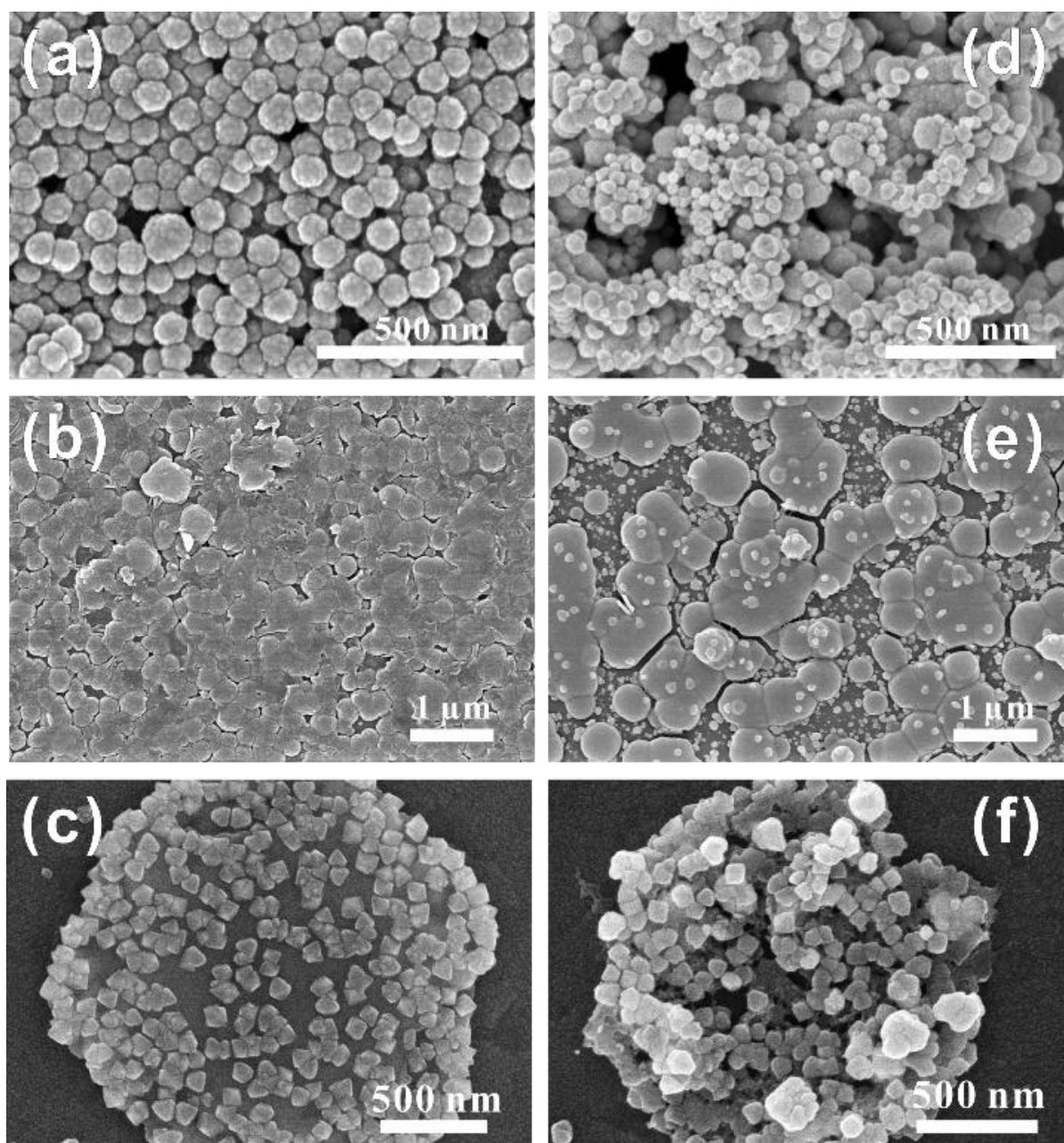


Figure 1. SEM images of chemical-bath-deposited (a) CdS, (b) ZnS, and (c) PbS nanoparticles and subsequently grown Au nanoparticles for 3 h (d) Au-CdS, (e) Au-ZnS, and Au-PbS.

3.2. Growth of Au nanoparticles

After the MS/ITO (M = Cd, Zn, and Pb) slides were immersed in the Au growth solution containing HAuCl_4 and CTAC at pH 6.0 for several hours, the films became darker with a brown-red coloration with the increase of growth time. The SEM images (Figure 1(d)-(f)) show clearly that a number of small nanoparticles were formed on the surface of CdS, ZnS, and PbS thin films. The XRD results (Figure 2) support that the formation of metallic gold on the surface of the slides.

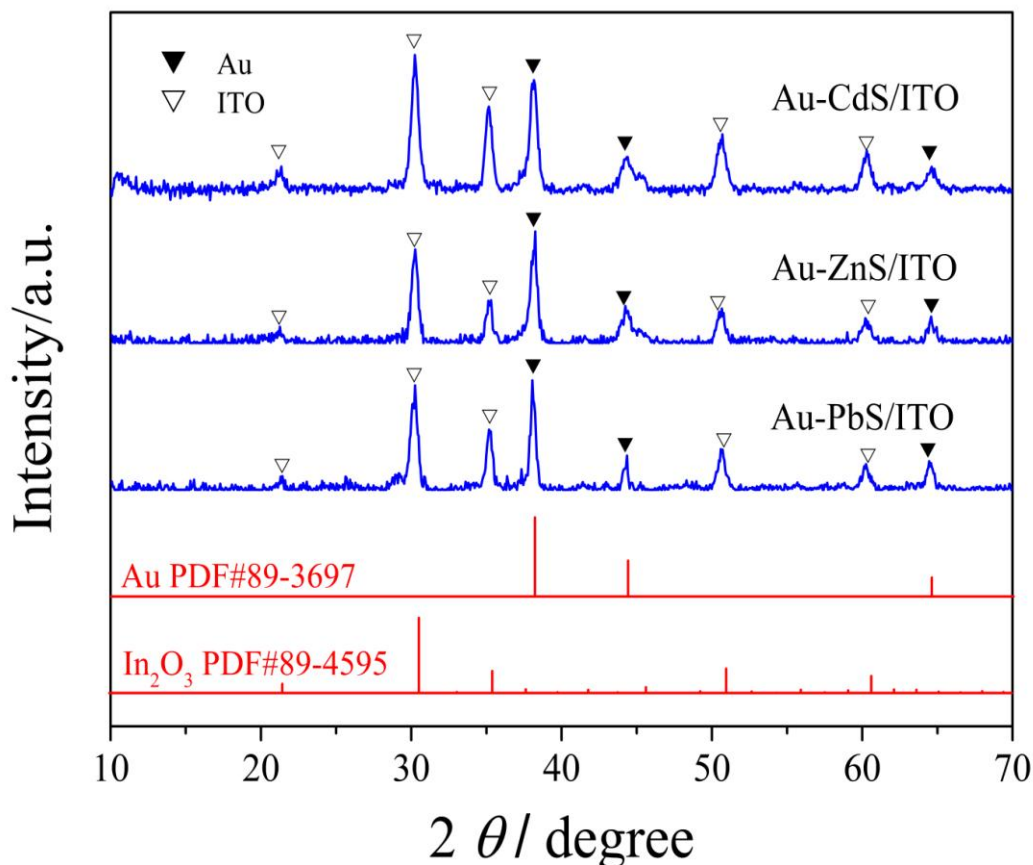


Figure 2. XRD of the growth of Au nanoparticles on CdS, ZnS, and PbS nanoparticles.

TEM provides much more details about the gold-semiconductor structure. For instance, two kinds of contrast regions, dark and gray, can be seen in all TEM images of Au-CdS microstructure (Figure 3). Because the electron scattering of Au is much stronger than that of CdS, the dark contrast is mainly from Au grains. The high-resolution TEM (HRTEM) image of the Au nanoparticle (Figure 3b) shows the interplanar distance of 0.232 nm, corresponding to the (111) plane of the face-centered cubic (fcc) lattice. The measured lattice spacing on gray grains of 0.245 nm is in good agreement with the (101) interplanar distance of the hexagonal CdS.

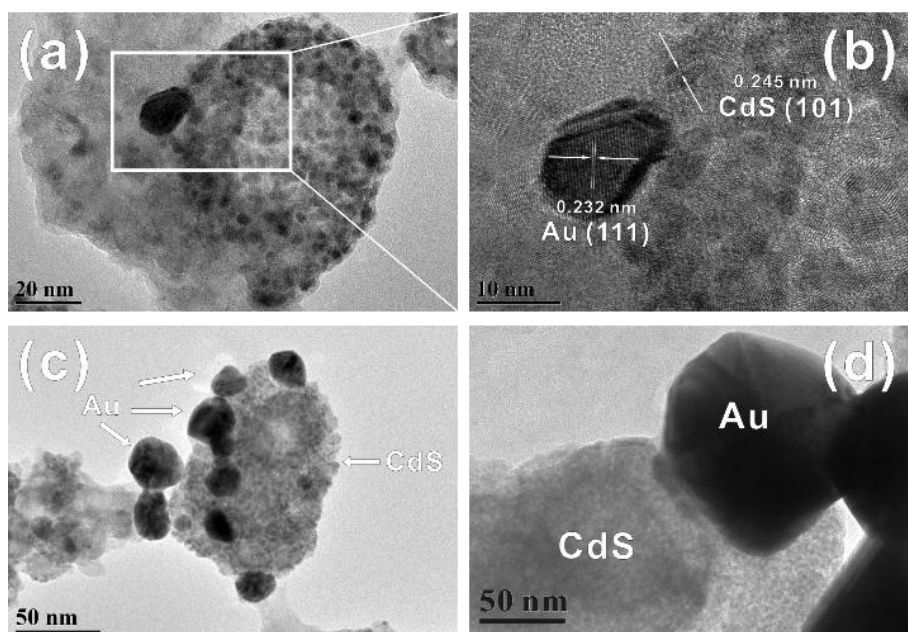


Figure 3. TEM and HRTEM images of the growth of Au nanoparticles on CdS grains.

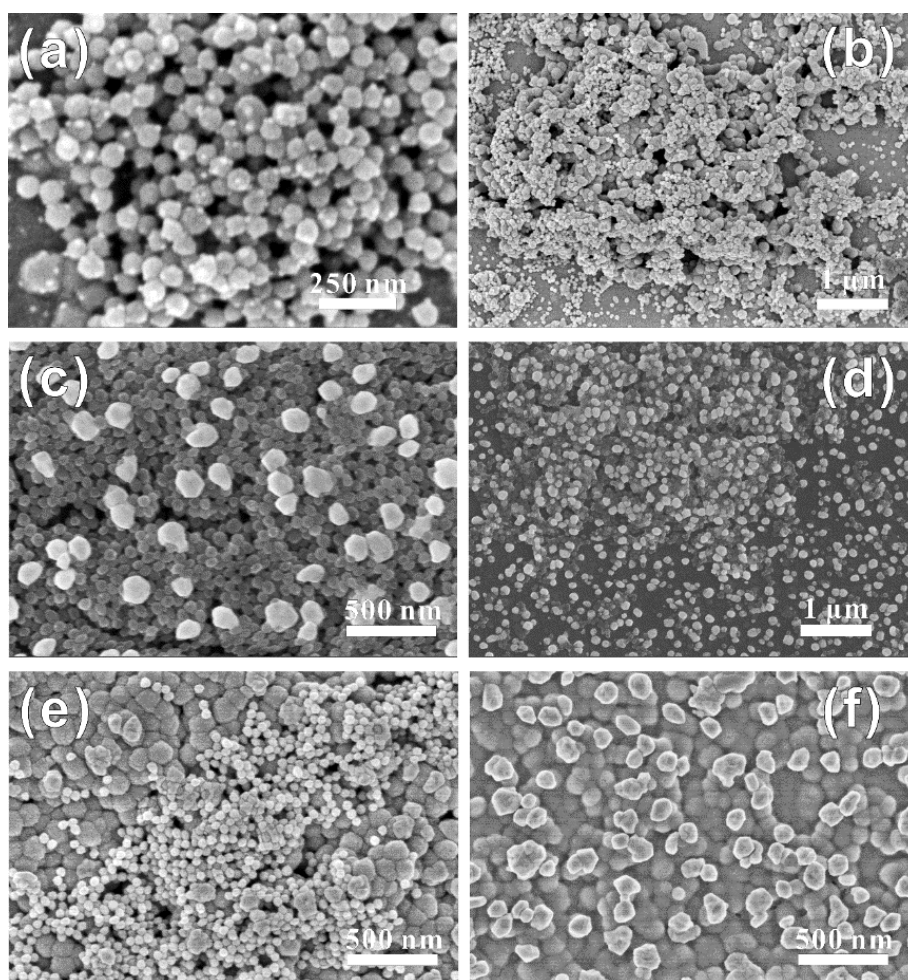
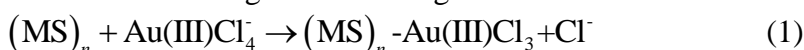


Figure 4. Growing gold onto CdS for 3 h at an Au(III) concentration of (a) 2.4, (b) 4.7, (c) 9.4 and (d) 19.2 mM. Growing gold for (e) 3 and (f) 12 h at 4.7 mM of Au(III).

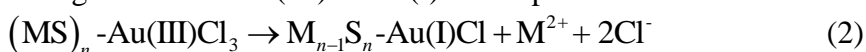
We investigated the effect of Au(III) concentration and growth time on the size of Au nanoparticles (Figure 4). Our results support that the greater Au(III) concentration or the longer growth time leads to larger size of Au nanoparticles. Small Au nanoparticles (15~20 nm) were observed on the surface of CdS grains after 3 h of growth at an Au(III) concentration of 2.4 mM (Figure 4a). When the concentrations of Au(III) increased to 4.7 and 9.4 mM, the diameters of Au nanoparticles were enlarged to approximately 50 and 115 nm, respectively (Figure 4b and d). However, increasing the Au(III) concentration up to 19.2 mM, there was no significant increase in the size of Au nanoparticles (~120 nm) (Figure 4e). We also investigated the effect of growth time on the diameter of Au nanoparticles. Figure 4e and 4f suggest that if the other growth conditions were kept unchanged (4.7 mM of Au(III)), the sizes of Au nanoparticles were enlarged from 50 to 100 nm while the growth time increased from 3 to 12 h.

3.3. The mechanism of the growth of Au nanoparticles

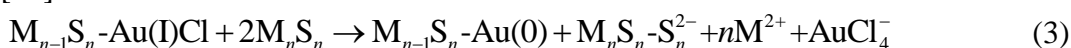
It is well known in mineralogy that gold species spontaneously deposit on sulfide minerals to form “invisible” gold[22]. A number of studies support the precipitation of gold involves the surface reduction and adsorption. According to the previous and our studies, we suggest a possible mechanism for spontaneous growth of Au nanoparticles onto MS (M = Cd, Zn, and Pb) thin films. This process may undergo an adsorption/reduction process[23]. In the first step, AuCl_4^- adsorbed onto the surface of MS thin films due to strong Au-S bonding.



Previous studies suggested that gold deposition on sulfide minerals involves oxidation of the mineral surface and spontaneous reduction of Au(III) to Au(I) and Au(0)[22-29]. The first possible reduction of gold is from Au(III) to Au(I) accompanied with the oxidation of S^{2-} in MS.



For the reduction of Au(I) to Au(0), we considered the disproportionation of Au(I) to Au(III) and Au(0), which can lead to the formation of metal vacancies and polysulphide (S_n^{2-}) adsorbed to the surface[25].



These equations reveal that metal ions (M^{2+}) are released into solution. To confirm the release of metal ions, we analysed the solutions after the Au growth by using anodic stripping voltammetry with a mercury-film electrode. The metal ions (Cd^{2+} , Zn^{2+} , and Pb^{2+}) were detected, which supports the release of M^{2+} from the MS films.

Once formed at the surface of MS films, Au(0) atoms can undergo surface diffusion and tend to coagulate to dimers and islands. These Au dimers and islands are extremely reactive and can catalyse the reduction of Au(III) onto the surface to form larger Au nanoparticles.

Usually, in a typical synthesis of Au nanoparticles, citrate or other reducing agents are used to reduce Au(III) to Au(0) [30-32]. Willner and co-workers have developed a biocatalytic approach for

the growth of Au nanoparticles. In this approach, H_2O_2 was used to reduce Au(III) in the presence of Au nanoseeds[15-17]. The more H_2O_2 is added, the more Au nanoparticles are formed.

However, our findings showed a completely opposite result, in that the addition of H_2O_2 appeared to inhibit the Au growth onto the MS surface, rather than promote it. We used both spectroscopic and electrochemical methods to detect the amount of the grown Au onto the MS films. The spectroscopic method is based on the measurement of the plasmon absorption band of Au nanoparticles. The other approach to detect the Au amounts is to measure the cathodic current of anodized Au at 1.35 V in a H_2SO_4 solution. This method may avoid inaccuracy in absorbance measurement caused by Au nanoparticles aggregation. These two methods yielded identical results that the absorbance and cathodic current are linearly decreased to the H_2O_2 concentration, supporting that the addition of H_2O_2 inhibits the Au nanoparticles growth.

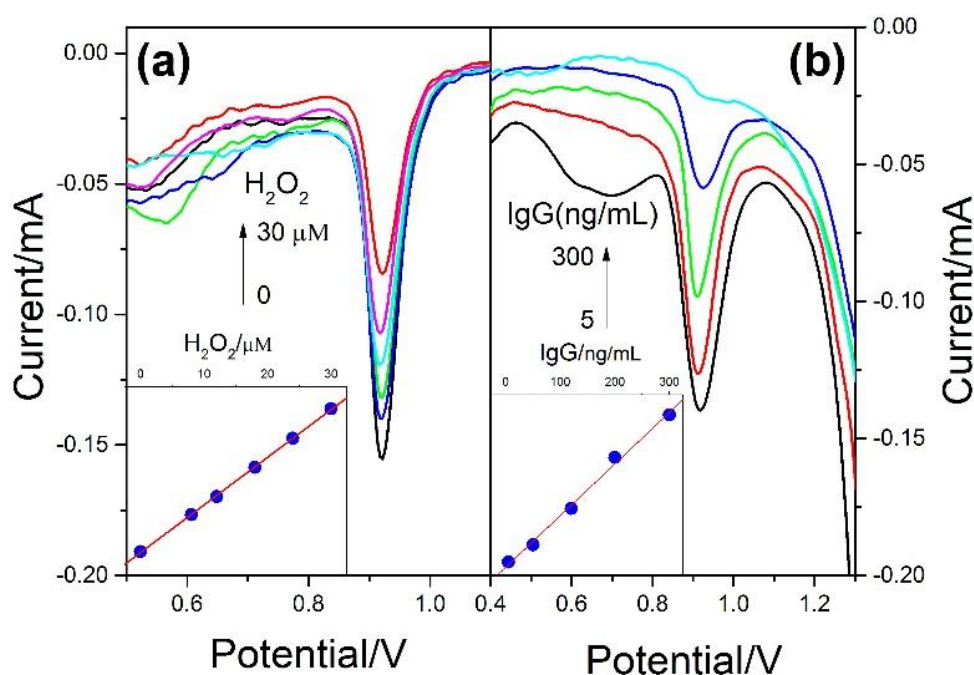
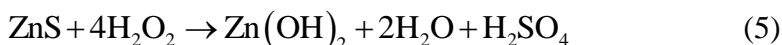


Figure 5. The differential pulse voltammograms of (a) CdS/ITO electrodes with increasing H_2O_2 and (b) immunosensors with increasing IgG in the Au growth solutions.

We suggested that the inhibition effect of H_2O_2 is mainly caused by the reactions between MS and H_2O_2 . According to Jennings et al, the reactions of metal sulfide with H_2O_2 are presented in Eq. 4 and 5[33].



As seen in Equations 4 and 5, the consumption of metal sulfide results in difficulty in the adsorption and reduction of Au(III), and eventually led to inhibit the Au growth.

3.4. The fabrication of immunosensors and assay procedure

H_2O_2 is a general enzymatic product of oxidases and a substrate of peroxidases, which is important in enzyme assays and enzyme-linked immunosorbent assay[18]. After demonstrating the inhibition effect of H_2O_2 on the Au growth, we adapted this process as the signal generation mechanism for enzyme immunoassays. To this end, we developed an enzyme-linked sandwich immunoassay for the detection of human immunoglobulin G (IgG) as a model analyte.

In our procedure (Figure 6), we use the glucose oxidase (GOx) labeled antibody to generate hydrogen peroxide that inhibits the Au growth on CdS films, thereby decreasing the cathodic current at 0.9 V. Firstly, the CdS thin film was deposited on the ITO electrode, followed by adsorption of goat-anti-human IgG antibody (Ab1) and blocking with bovine serum albumin. Subsequently, the electrode was incubated in a solution containing various concentrations of IgG. We used monoclonal mouse-anti-human IgG antibody (Ab2) and GOx-conjugated Au nanoparticles (GOx-Ab2-AuNPs) as the secondary antibody for a sandwich configuration[12]. GOx was introduced on the electrode surface by forming an antibody–antigen–antibody conjugate sandwich. Afterwards, the electrode was incubated in the solution containing $AuCl_4^-$ and glucose. As discussed previously, Au(III) ions can spontaneously reduce to Au nanoparticles onto the CdS surface. However, in the presence of GOx that produces H_2O_2 by catalyzing the oxidation of glucose, the Au growth is inhibited. Consequently, the cathodic current at 0.9 V decreased with IgG (Figure 5b), which supports the signal generation mechanism for the enzyme immunoassays. This immunosensor can detect IgG as low as 1.5 ng/mL.

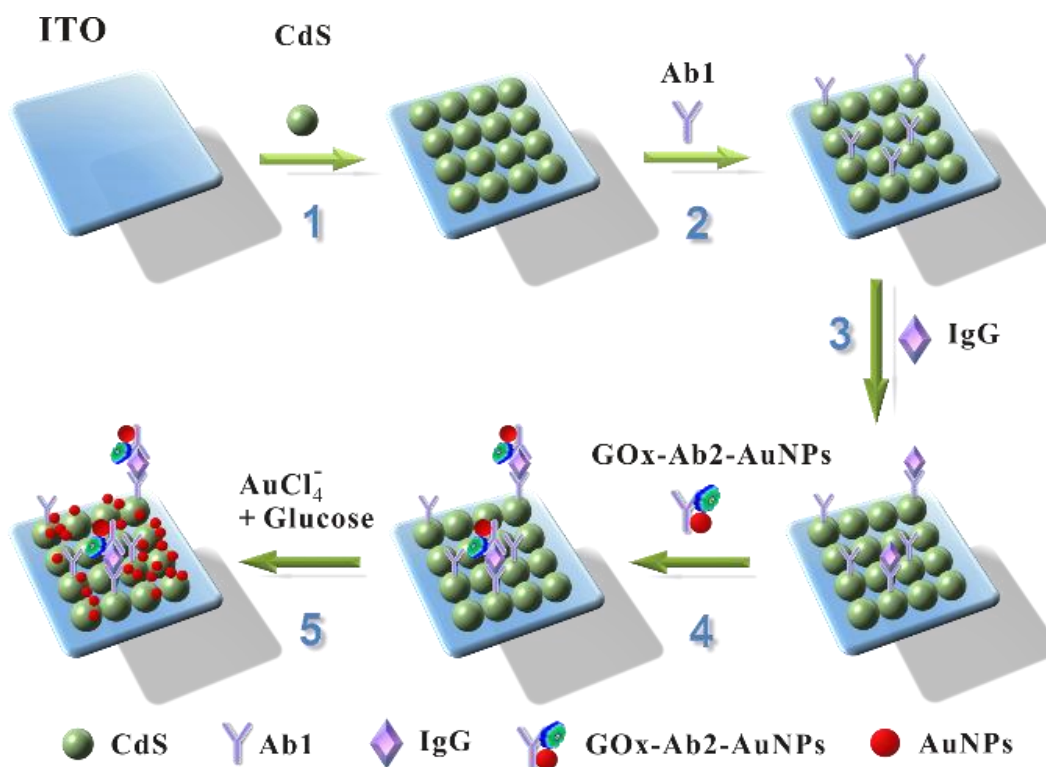


Figure 6. Scheme of immunosensor fabrication and assay procedure.

4. CONCLUSIONS

We developed a facile method to fabricate Au-CdS (ZnS or PbS) nanocomposites by spontaneous growth of Au onto the surface of the metal sulfide nanoparticles. A possible mechanism was proposed for spontaneous growth of Au nanoparticles. In the first step, AuCl_4^- adsorbed onto the surface of metal sulfide due to strong Au-S bonding. Subsequently, gold was deposited on sulfide minerals, which involves oxidation of the mineral surface and spontaneous reduction of Au(III) to Au(I) and Au(0). Once formed at the surface of MS films, Au(0) atoms can undergo surface diffusion and tend to coagulate to dimers and islands. These Au dimers and islands are extremely reactive and can catalyze the reduction of Au(III) onto the surface to form larger Au nanoparticles.

Furthermore, our findings showed that H_2O_2 appeared to inhibit the Au growth onto the MS surface. Accordingly, we developed an enzyme-linked sandwich immunoassay for the detection of IgG. This immunosensor can detect IgG as low as 1.5 ng/mL.

ACKNOWLEDGEMENTS

This work was financially supported by National Natural Science Foundation of China (20905016, 21265005), Guangxi Natural Science Foundation (0991082) and the project of high level innovation team and outstanding scholar in Guangxi colleges and universities.

References

1. B. F. Mangelson, M. R. Jones, D. J. Park, C. M. Shade, G. C. Schatz and C. A. Mirkin, *Chem. Mater.*, 26 (2014) 3818
2. W. W. Zhan, Q. Kuang, J. Z. Zhou, X. J. Kong, Z. X. Xie and L. S. Zheng, *J. Am. Chem. Soc.*, 135 (2013) 1926
3. R. Marschall, *Adv. Funct. Mater.*, 24 (2014) 2421
4. H. Wang, L. Zhang, Z. Chen, J. Hu, S. Li, Z. Wang, J. Liu and X. Wang, *Chem. Soc. Rev.*, 43 (2014) 5234
5. M. Li, X.-F. Yu, S. Liang, X.-N. Peng, Z.-J. Yang, Y.-L. Wang and Q.-Q. Wang, *Adv. Funct. Mater.*, 21 (2011) 1788
6. K. Qian, B. C. Sweeny, A. C. Johnston-Peck, W. Niu, J. O. Graham, J. S. DuChene, J. Qiu, Y. C. Wang, M. H. Engelhard, D. Su, E. A. Stach and W. D. Wei, *J. Am. Chem. Soc.*, 136 (2014) 9842
7. G. Menagen, J. E. Macdonald, Y. Shemesh, I. Popov and U. Banin, *J. Am. Chem. Soc.*, 131 (2009) 17406
8. J. Shi, *Chem. Rev.*, 113 (2013) 2139
9. U. Banin, Y. Ben-Shahar and K. Vinokurov, *Chem. Mater.*, 26 (2014) 97
10. E. Khon, A. Mereshchenko, A. N. Tarnovsky, K. Acharya, A. Klinkova, N. N. Hewa-Kasakarage, I. Nemitz and M. Zamkov, *Nano Lett.*, 11 (2011) 1792
11. N. Zhou, J. Wang, T. Chen, Z. Yu and G. Li, *Anal. Chem.*, 78 (2006) 5227
12. H. Pan, D. Li, J. Li, W. Zhu and L. Fang, *Int. J. Electrochem. Sci.*, 7 (2012) 12883
13. Y. Weizmann, F. Patolsky and I. Willner, *Analyst*, 126 (2001) 1502
14. I. Willner, F. Patolsky, Y. Weizmann and B. Willner, *Talanta*, 56 (2002) 847
15. I. Willner, R. Baron and B. Willner, *Adv. Mater.*, 18 (2006) 1109
16. Y. M. Yan, R. Tel-Vered, O. Yehezkeli, Z. Cheglakov and I. Willner, *Adv. Mater.*, 20 (2008) 2365
17. M. Zayats, R. Baron, I. Popov and I. Willner, *Nano Lett.*, 5 (2005) 21
18. R. de la Rica and M. M. Stevens, *Nat. Nanotechnol.*, 7 (2012) 821

19. A. Kariper, E. Güneri, F. Göde, C. Gümüş and T. Özpozan, *Mater. Chem. Phys.*, 129 (2011) 183
20. G. Hodes, *Chemical solution deposition of semiconductor films*, Marcel Dekker, New York, (2002)
21. H. Khallaf, I. O. Oladeji, G. Chai and L. Chow, *Thin Solid Films*, 516 (2008) 7306
22. L. M. Maddox, G. M. Bancroft, M. J. Scaini and J. W. Lorimer, *Am. Mineral.*, 83 (1998) 1240
23. U. Becker, M. F. Hochella and D. J. Vaughan, *Geochim. Cosmochim. Acta*, 61 (1997) 3565
24. Y. L. Mikhlin and A. S. Romanchenko, *Geochim. Cosmochim. Acta*, 71 (2007) 5985
25. M. J. Scaini, G. M. Bancroft and S. W. Jsnipe, *Geochim. Cosmochim. Acta*, 61 (1997) 1223
26. Y. Mikhlin, A. Romanchenko, M. Likhatski, A. Karacharov, S. Erenburg and S. Trubina, *Ore Geol. Rev.*, 42 (2011) 47
27. R. Murphy and D. Strongin, *Surf. Sci. Rep.*, 64 (2009) 1
28. H. C. Choi, M. Shim, S. Bangsaruntip and H. Dai, *J. Am. Chem. Soc.*, 124 (2002) 9058
29. J. R. MYCROFF, G. M. BANCROFT, N. S. MCINTYRE and J. W. LORIMER, *Geochimica et Cosmochimica Acta*, 59 (1995) 3351
30. S. Guo and E. Wang, *Nano Today*, 6 (2011) 240
31. X. Huang, S. Neretina and M. A. El-Sayed, *Adv. Mater.*, 21 (2009) 4880
32. M.-C. Daniel and D. Astruc, *Chem. Rev.*, 104 (2003)
33. S. R. Jennings, D. J. Dollhopf and W. P. Inskeep, *Appl. Geochem.*, 15 (2000) 235

© 2016 The Authors. Published by ESG (www.electrochemsci.org). This article is an open access article distributed under the terms and conditions of the Creative Commons Attribution license (<http://creativecommons.org/licenses/by/4.0/>).